Eur Spine J (2012) 21:920–929
DOI 10.1007/s00586-011-2119-5

ORIGINAL ARTICLE

# The effect of standard and low-modulus cement augmentation on the stiffness, strength, and endplate pressure distribution in vertebroplasty

**Michael Kinzl · Lorin M. Benneker · Andreas Boger · Philippe K. Zysset · Dieter H. Pahr**

Received: 7 July 2011 / Revised: 27 October 2011 / Accepted: 6 December 2011 / Published online: 15 December 2011


**Abstract**
*Purpose* Vertebroplasty restores stiffness and strength of fractured vertebral bodies, but alters their stress transfer. This unwanted effect may be reduced by using more compliant cements. However, systematic experimental comparison of structural properties between standard and low-modulus augmentation needs to be done. This study investigated how standard and low-modulus cement augmentation affects apparent stiffness, strength, and endplate pressure distribution of vertebral body sections.
*Methods* Thirty-nine human thoracolumbar vertebral body sections were prepared by removing cortical endplates and posterior elements. The specimens were scanned with a HR-pQCT system and loaded in the elastic range. After augmentation with standard or low-modulus cement they were scanned again and tested in two steps. First, the contact pressure distribution between specimen and loading plates was measured with pressure-sensitive films. Then, they were loaded again in the elastic range and compressed until failure. Apparent stiffness was compared before and after augmentation, whereas apparent strength of augmented specimens was compared to a non-augmented reference group.
*Results* Vertebral body sections with fillings connecting both endplates were on average 33% stiffer and 47% stronger with standard cement, and 27% stiffer and 30% stronger with low-modulus cement. In contrast, partial fillings showed no significant strengthening for both cements and only a slight stiffness increase (<16%). The averaged endplate pressure above/below the cement was on average 15% lower with low-modulus cement compared to standard cement.
*Conclusion* Augmentation connecting both endplates significantly strengthened and stiffened vertebral body sections also with low-modulus cement. A trend of reduced pressure concentrations above/below the cement was observed with low-modulus cement.

**Keywords** Vertebroplasty · Low-modulus · PMMA · Cement · Vertebral body · Mechanical properties

M. Kinzl (✉) · D. H. Pahr
Institute of Lightweight Design and Structural Biomechanics, Vienna University of Technology, Gusshausstrasse 27-29, 1040 Vienna, Austria
e-mail: kinzl@ilsb.tuwien.ac.at

L. M. Benneker
Department of Orthopaedic Surgery, University of Bern, Inselspital, Bern, Switzerland

A. Boger
Ansbach University of Applied Sciences, Ansbach, Germany

P. K. Zysset
Institute of Surgical Technology and Biomechanics, University of Bern, Bern, Switzerland

## Introduction

Vertebroplasty is able to restore vertebral body stiffness and strength [1, 2], and most importantly leads to immediate and lasting pain relief [3]. Of concern is the increased risk of adjacent vertebral body fractures observed in clinical [4, 5] and experimental studies [6–8]. Although a recent randomized controlled trial comparing vertebroplasty to conservative treatment [9] found no significant difference in adjacent-level fracture incidence, clinically used poly-methyl-methacrylate (PMMA) cements caused marked changes in load transfer. A pressure increase in the nucleus pulposus and a reduced inward deflection of the augmented endplate were observed following augmentation [10, 11]. One reason is that the elastic modulus of standard PMMA bone cements is one order of magnitude larger than the apparent elastic modulus of osteoporotic trabecular bone [12, 13], whereas low-modulus cement has a stiffness comparable to trabecular bone [14].

Such adapted cement materials better preserved the failure strength of augmented functional spine units compared to standard PMMA [7], because failure mostly occurred in the adjacent level. Chevalier et al. [15] showed numerically that a decreased elastic modulus of the cement reduced the stresses above/below the cement region while still strengthening the vertebral body. Shortcomings of this study were the purely numerical nature without experimental validation of the augmented finite element models and that only standard cement was injected. Both studies indicated advantages of more compliant cement materials, which could be beneficial in case of moderate fractures or prophylactic vertebroplasty where less strength increase is required. A systematic experimental comparison of strength, stiffness, and measured endplate load transfer between standard and low-modulus cement augmentation has not been published so far and is important for characterizing their biomechanical differences.

This requires well-designed testing setups to mimic the in vivo situation, because in vivo measurements are practically not possible. Several experimental setups were presented that allowed rotation of the upper loading plate during compression [16–18], which produces uniform loading of the specimen and better reproduces in vivo loading conditions than compression between parallel plates. However, in most studies [1, 15, 16, 18–20] the endplates were embedded, whereby experimental uncertainties in the measured displacements and stiffness values were introduced due to the compliance of the embedding material and its contact conditions with the bone. These uncertainties can be minimized by using vertebral body sections [17], which requires the removal of the endplates, but also allows measuring the load transfer near the endplate.

Since the comparison of structural properties after augmentation is strongly influenced by the filling pattern [15, 25], experimental results need to be interpreted in consideration of this factor. To quantify the effectiveness of standard and low-modulus cement augmentation accurately, increases in stiffness and strength need to be compared either to the non-augmented state for the same vertebral body or to a matched non-augmented reference group.

In this sense, our objectives were to compare the mentioned structural properties as well as endplate pressure distributions between augmentation with a clinically used standard cement and with an experimental low-modulus cement.

## Methods

### Specimen preparation

Thirty-nine human thoracolumbar vertebral bodies (T9–L5) were obtained from five female and six male donors (age 44–82). All soft tissues and the intervertebral disks were removed (Fig. 1). The cortical endplates were removed in small cutting steps perpendicular to the major trabecular orientation with a diamond-coated band saw (300 CP, Exakt GmbH, Norderstedt, Germany) until all cortical bone of the endplate was removed (remaining height $16.5 \pm 2.6$ mm). After removing the posterior elements, the cranial/caudal cutting surfaces were polished with silicon carbide paper (P1000, PM5, Logitech Ltd, Glasgow, Scotland) to obtain plane and parallel surfaces. All procedures were performed under constant water irrigation. The prepared vertebral body sections were assigned to the standard and low-modulus cement groups, such that the mean bone volume fraction (BV/TV) computed from the HR-pQCT images as described below, age, gender, and spinal levels were matched.

### Ex vivo vertebroplasty

Standard vertebroplasty cement (Vertecem, Synthes GmbH, Oberdorf, Switzerland) was prepared according to the manufacturer's instructions. The same was used for the low-modulus cement, but 50% of the liquid monomer phase was replaced with NMP (1-methyl-2-pyrrolidone, Sigma Aldrich, Buchs, Switzerland) as described in [21]. The cranial/caudal surfaces were covered with hard plastic disks. Twenty specimens were augmented with standard cement and 19 with low-modulus cement via a unipedicular approach by an experienced surgeon under continuous radiographic monitoring. The cement was injected until either leakage was observed or a filling connecting both endplates was achieved. After curing of the cement, the cranial/caudal surfaces were polished again (<0.1 mm was removed from each side). The elastic moduli and yield stress of the pure standard and low-modulus cement were determined from compression test of 90 cylindrical cement samples (8 mm diameter, 12 mm height), which were prepared from the remaining cement.

### HR-pQCT scanning

The vertebral body sections were scanned with a HR-pQCT system (60 kV, 900 µA, 82 µm voxel size, XtremeCT, Scanco Medical AG, Zürich, Switzerland) before augmentation to obtain the bone morphology and after augmentation to obtain the filling patterns. The specimens were placed in a custom-made Plexiglas chamber filled

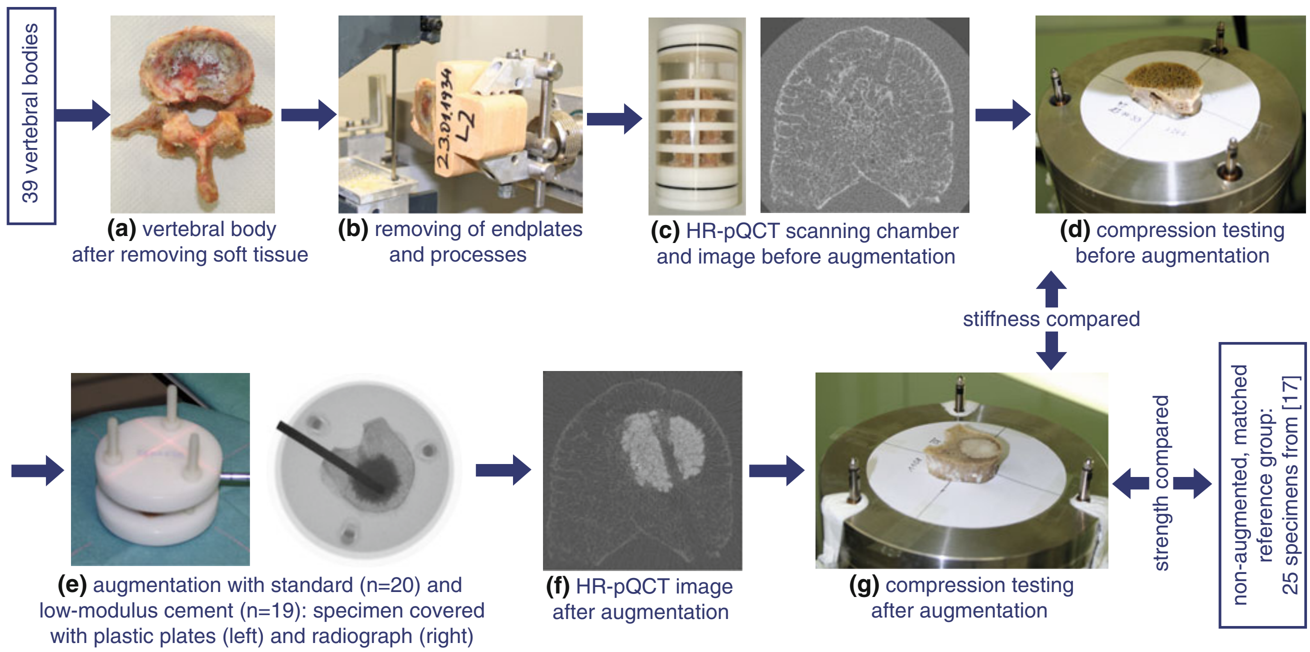


**Fig. 1** Overview of the specimen preparation, mechanical testing and CT scanning steps

with 0.9% saline solution. Air bubbles were removed using a vacuum chamber.

## Image processing

HR-pQCT images before augmentation were segmented (Fig. 2, left) using a Laplace–Hamming filter and a fixed 40% threshold value [22]. Outer and trabecular bone masks were extracted from the segmented images using closing and fill operations [23]. Masks of the cement region (Fig. 2, right) were extracted from the augmented HR-pQCT images using a fixed threshold value, which was determined by visual inspection. All images were registered using the software ITK to be able to overlay them (Fig. 2f). Cement volume was defined as the volume of the cement mask minus the included bone volume. The total BV/TV was computed for each specimen from the segmented HR-pQCT image and the outer bone mask.

## Mechanical tests

Specimens were immersed in 0.9% saline solution for at least 2 h before testing and were carefully positioned on the machine. Positioning sheets containing the projected frontal and sagittal plane as well as the shape of the vertebral body sections (Fig. 3b) were prepared. The projections of the frontal and sagittal planes were aligned with reference markers on the loading plate, such that the loading axis was shifted 5% of the anterior–posterior dimension (*h*) from the projected center of mass in the anterior direction. This shift is sufficient to produce anterior wedge-shaped fractures [17]. The same set of positioning sheets was used for all testing steps. Further details are given in [17].

A servohydraulic testing machine (Mini-Bionix, MTS system, Eden Prairie, MN, USA) was used to compress the specimens. Rotation of the upper loading plate was allowed by means of a ball joint (Fig. 3a) and both loading surfaces were sandblasted to increase friction. Three displacement sensors (LVDTs, WA20, HBM, Darmstadt, Germany) recorded the axial displacements at three points of the loading plate. The axial force was measured by means of a 100 kN load cell (U3 force transducer, HBM, Darmstadt, Germany).

Before augmentation, the specimens were monotonically compressed (rate 2.5 mm/min) in the elastic range with a maximum force of 800–1,200 N (depending on the specimen size) after ten low-load preconditioning cycles (amplitude 60 N). After augmentation, all specimens were tested again in two steps. During the first step, pressure-sensitive colour films (Prescale LLW, Fujifilm, Düsseldorf, Germany) were placed between the specimens and both loading plates and a constant load of 1,000 N was applied for 10 s (manufacturer's instruction). In a second step, the specimens were preconditioned as before augmentation and then compressed monotonically until failure using the same rate.

Axial displacement of the loading plate was obtained by averaging the three LVDTs displacements. The mean cross-sectional area (mean CSA) of each specimen was

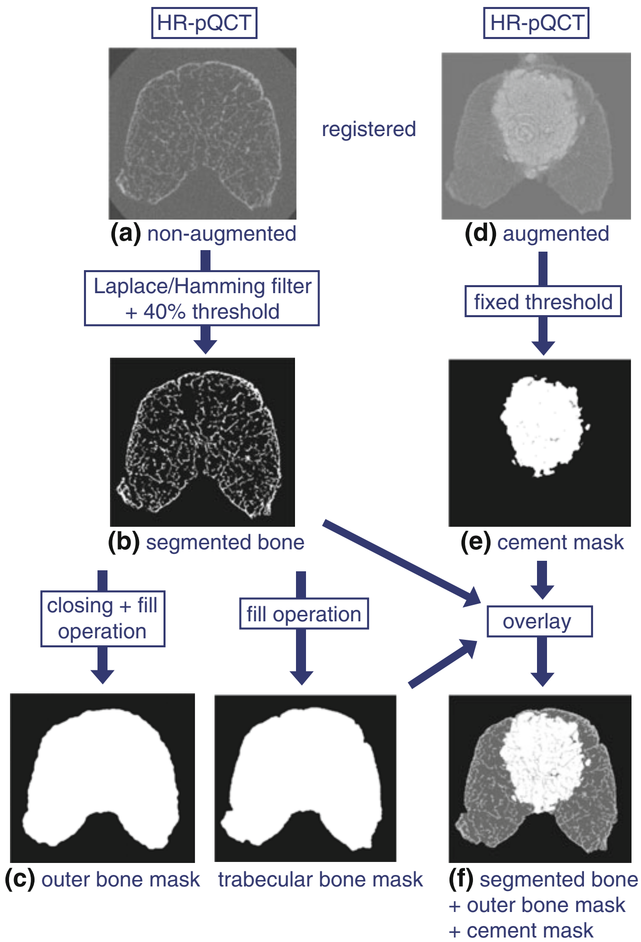


**Fig. 2** Image processing steps performed on the HR-pQCT images of non-augmented (*left*) and augmented (*right*) vertebral body sections. The non-augmented images (**a**) were segmented (**b**). Outer and trabecular bone masks were extracted (**c**). From the augmented images (**d**) masks for the cement (**e**) were segmented using a fixed threshold. All images were registered to overlay the segmented images and the masks (**f**)

defined as the volume of the outer bone mask divided by the height. Apparent stiffness was computed as the maximum slope (Fig. 4) in the linear range of the "load-displacement" curve multiplied by the specimen height divided by the mean CSA. Apparent strength was computed as the first load maximum divided by the mean CSA.

## Non-augmented reference group

Since the 39 specimens were only tested in the elastic range before augmentation to obtain the stiffness, augmented apparent strength had to be compared to a non-augmented reference group from another study [17]. In this previous study 37 thoracolumbar vertebral body sections (T12–L5, age 44–82) from seven male and three female spines were compressed until failure using the same testing and

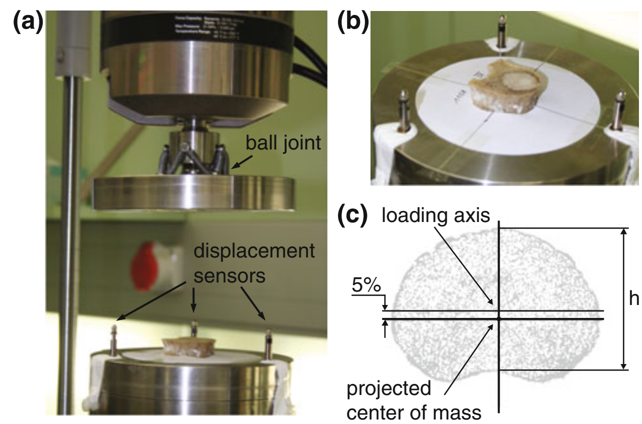


**Fig. 3** Compression testing setup for vertebral body sections (**a**). The upper loading plate was allowed to rotate by means of a ball joint and its position was measured with three displacement sensors. Specimens were aligned to reference markers (**b**) of the setup with positioning sheets (**c**). The loading axis was moved 5% of the width (*h*) from the projected center of mass in the anterior direction. The contrast of the reference markers was increased to improve visibility

preparation procedure. From these 37 specimens, 25 were selected such that the regression equation of non-augmented apparent stiffness over BV/TV was matched to the current study (slope: $p = 0.958$, intercept: $p = 0.965$). In addition, mean apparent stiffness ($p = 0.584$), age, and gender were matched between the two groups. Since apparent strength and stiffness were well correlated ($R^2 = 0.835$) for the reference group, this matching of regression equations and mean apparent stiffness provided similar apparent strength distributions in both groups.

## Pressure-sensitive films

Specimens with partial fillings or others presenting insufficient surface quality were excluded from the film analysis. The cranial/caudal films of the remaining 30 specimens were scanned as grey-value images (300 dpi, 8 bit grey-value bitmap image, HP Scanjet G2710, Hewlett-Packard, Palo Alto, CA, USA). Since the colour intensity of the film corresponds to the contact pressure level, a calibration function between pressure and grey value was determined as follows. A calibration sheet with 15 calibration points (applied pressure levels 0.6–3.9 MPa) was prepared by loading the pressure-sensitive film on the servohydraulic testing machine with a polished aluminium rod at constant load for 10 s. The calibration sheet was scanned as grey-value image. Applied pressure values and average grey values were determined for each calibration point using the software GODAV (Klaus Hoffmann, IKL, Vienna University of Technology, Vienna, Austria). The calibration function was defined as a piecewise-linear function connecting the determined values. The cranial/caudal grey-value images were calibrated to obtain pressure

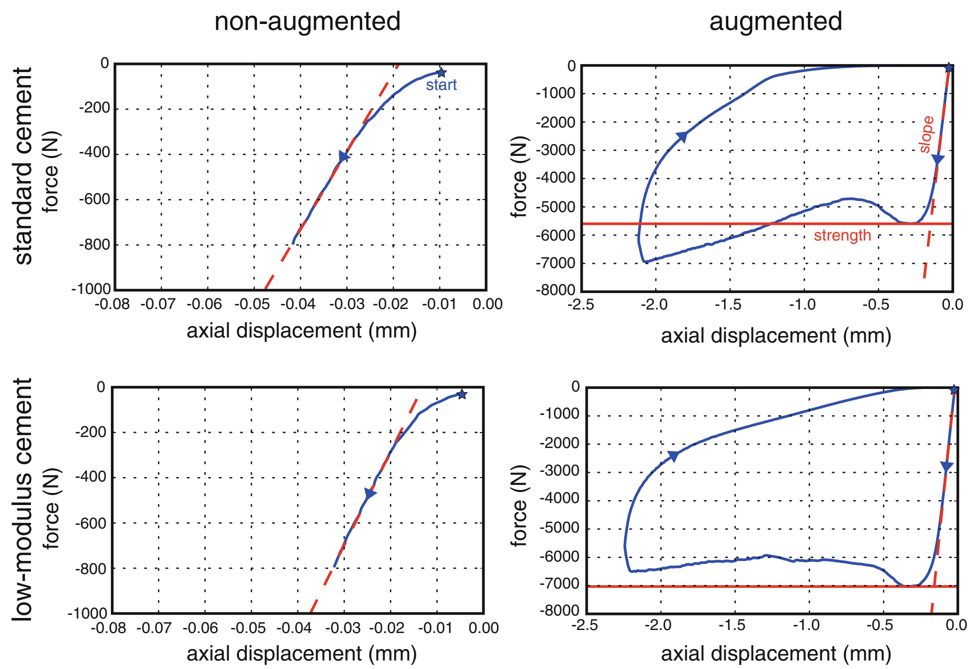


**Fig. 4** Typical load-displacement curves for a standard (*top*) and a low-modulus (*bottom*) cement specimen before and after augmentation. *Red lines* represent the slope (*dashed*) and strength (*solid*)

distributions and were overlaid with the cement and trabecular bone mask. The endplate pressure within the cement region (Fig. 2e) and the trabecular bone region (Fig. 2c) were averaged inside their respective mask.

### Statistical analysis

Correlation coefficients and regression equations were determined by using orthogonal regression [24]. Paired two-tailed Student's *t*-tests were performed to compare the mean apparent stiffness before and after augmentation. All other comparisons of means were based on unpaired two-tailed Student's *t*-tests. Statistical tests were performed at a probability level of 95%.

## Results

### Injected cement volumes

Cement distributions were classified for the standard/low-modulus cement group into fillings connecting both endplates (endplate-to-endplate filling: 15/16 specimens) and fillings touching only one endplate (partial filling: 5/3 specimens). Cement volumes ranged from 8 to 31% (1.9–6.0 ml) of the total specimen volume for endplate-to-endplate fillings and from 8 to 21% (2.0–4.4 ml) for partial fillings. Average cement volumes were significantly different ($p = 0.017$) between standard (3.4 ± 0.8 ml) and low-modulus cement (4.0 ± 0.9 ml), due to better injectability of the low-modulus cement.

### Cement samples

The tested elastic moduli of the pure standard and low-modulus cement were 2,306.0 ± 89.1 and 969.6 ± 70.2 MPa, respectively. The measured yield stress was 29.2 ± 2.6 MPa for the standard cement and 11.5 ± 1.3 MPa for the low-modulus cement.

### Vertebral body stiffness and strength

Typical load-displacement curves with slopes and maximum force are shown in Fig. 4 for two specimens before (left) and after augmentation (right) with standard (top) and low-modulus cement (bottom).

Apparent stiffness after augmentation was marginally larger with standard cement than with low-modulus cement ($p = 0.99$, power $= 0.52$). Specimens with endplate-to-endplate fillings were 33 and 27% stiffer compared to the non-augmented state ($p < 0.014$) with standard and low-modulus cement, respectively (Fig. 5). Only insignificant increase in stiffness was observed for partial fillings (standard cement: 8%, low-modulus cement: 16%).

Good correlations between apparent stiffness and BV/TV (Fig. 6) were found before augmentation ($R^2 = 0.67$ for standard cement and $R^2 = 0.75$ low-modulus cement) and after augmentation ($R^2 = 0.91$ for standard and $R^2 = 0.78$ low-modulus cement). The increase in apparent stiffness was not correlated with the degree of filling and the degree of filling was not correlated with BV/TV.

While partial fillings did not increase apparent strength, specimens with endplate-to-endplate fillings were 47 and

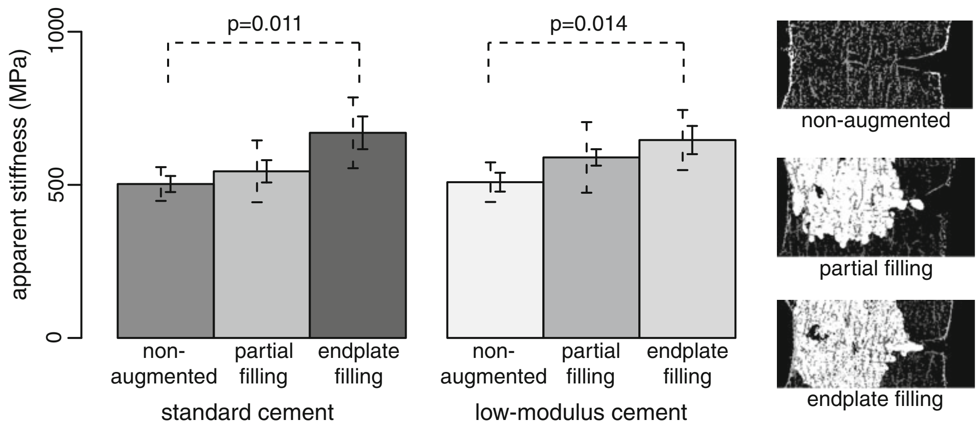


**Fig. 5** Apparent stiffness of vertebral body sections before and after augmentation for the standard and low-modulus cement group. Cement distributions were classified into fillings connecting both endplates (endplate-to-endplate fillings) and fillings contacting only one endplate (partial filling). *Error bars* indicate standard errors (*solid lines*) and confidence intervals (*dashed lines*)

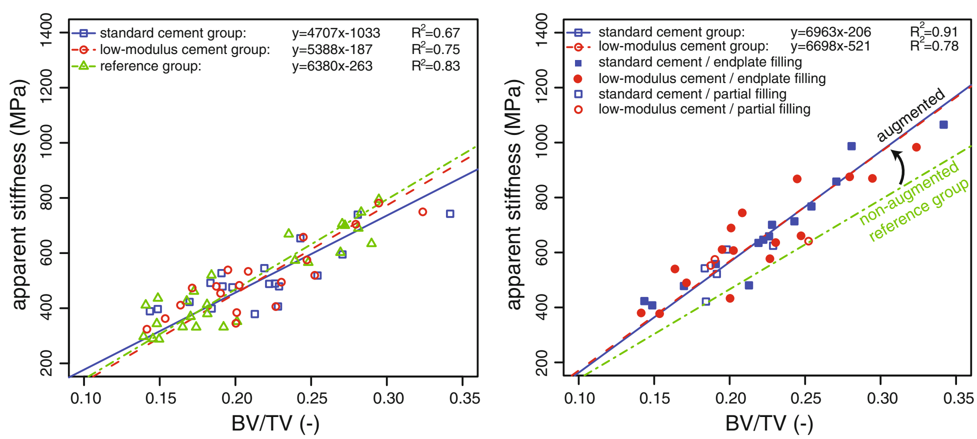


**Fig. 6** Correlation and regression equations of apparent stiffness over total BV/TV for non-augmented (*left*) and augmented (*right*) vertebral body sections. *Squares* represent the standard cement group, *circles* the low-modulus cement group and *triangles* the non-augmented reference group [20]. *Filled symbols* represent endplate-to-endplate fillings and *non-filled symbols* partial fillings (*right*)

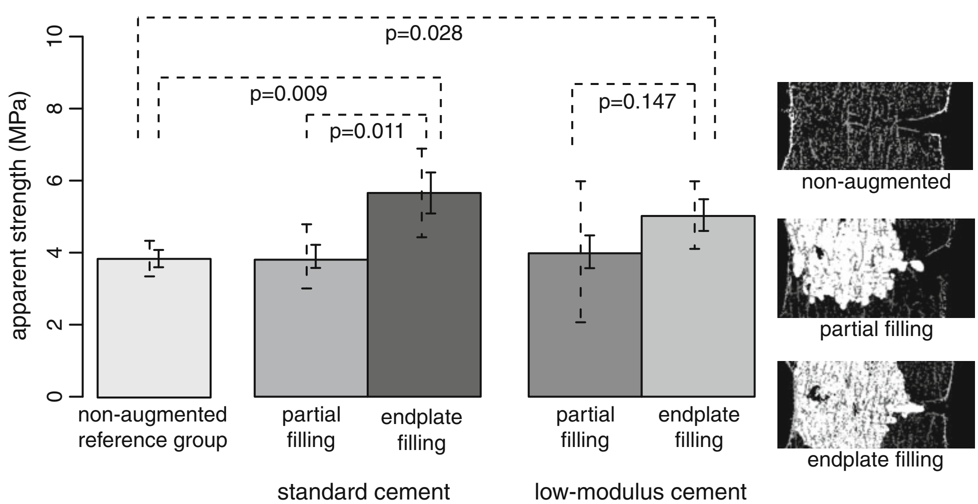


**Fig. 7** Apparent strength of vertebral body sections for the reference group [20], the standard and low-modulus cement group. Augmented specimens were classified in partial and endplate-to-endplate fillings. *Error bars* indicate standard errors (*solid lines*) and confidence intervals (*dashed lines*)

30% stronger than the non-augmented reference group for standard and low-modulus cement, respectively (Fig. 7). The increase in apparent strength was significant in both groups for endplate-to-endplate fillings, but somewhat smaller ($p = 0.60$, power = 0.50) with low-modulus cement compared to standard cement.

## Endplate pressure

The calibrated pressure-sensitive films (Fig. 8) clearly showed that the highest pressure occurred above/below the posterior wall and the cement region. The anterior cortical shell and trabecular bone near the cement were only

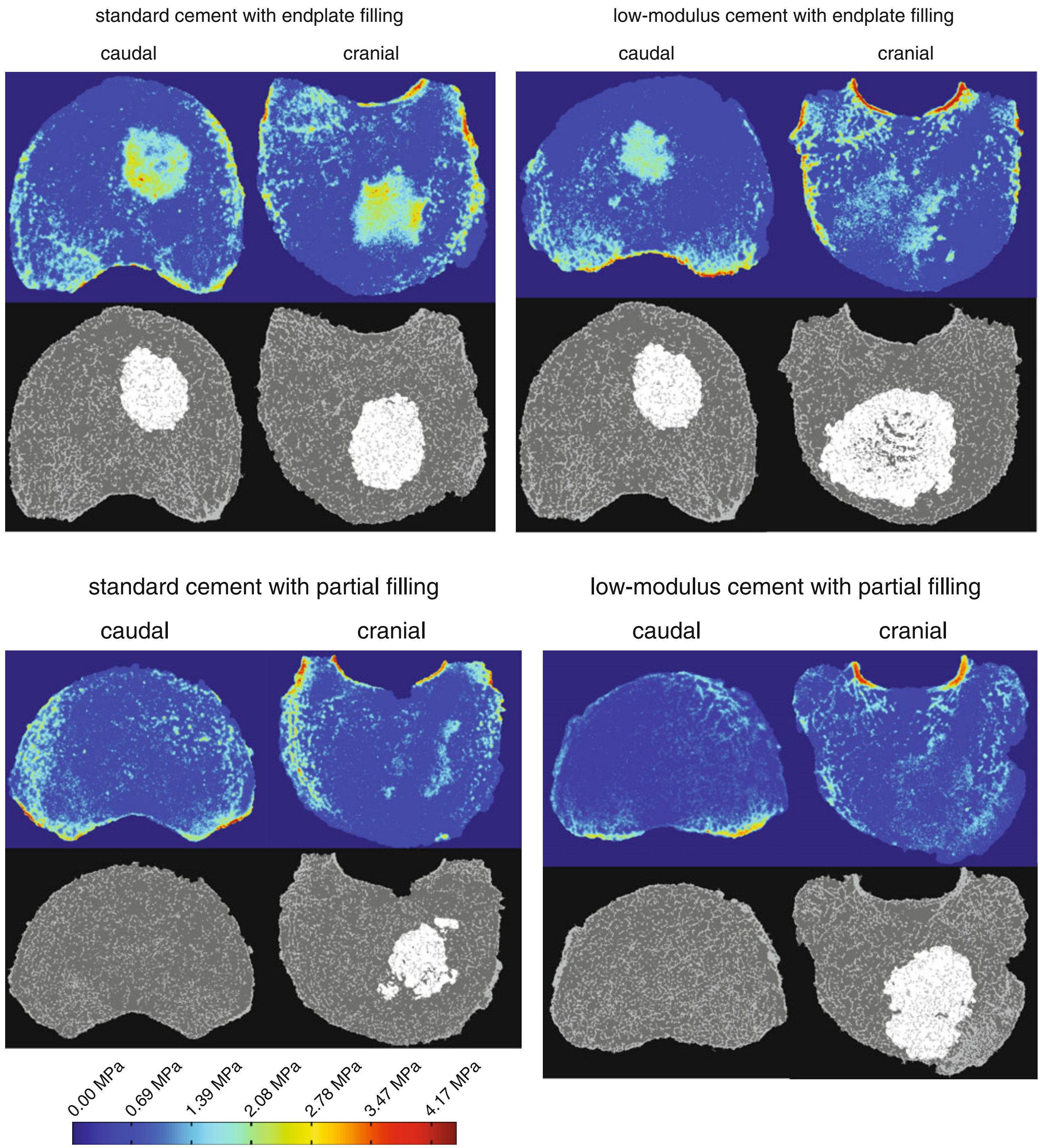


**Fig. 8** Calibrated and masked pressure-sensitive films for endplate fillings (*top*) and partial fillings (*bottom*) with standard (*left*) and low-modulus (*right*) cement and Laplace–Hamming filtered HR-pQCT images overlaid with the cement region (*white*) and the outer bone mask

minimally loaded. The ratio between the averaged pressure within the cement region and trabecular bone mask (Fig. 9) showed a pressure increase above/below the cement compared to the trabecular region. This pressure ratio was on average lower with the low-modulus cement (caudal film: 13.6%, $p = 0.17$; cranial film: 16.0%, $p = 0.09$) compared to the standard cement, but differences were not significant. Pressure distributions for the specimens with partial fillings, which were excluded from the above statistics, are also shown in Fig. 8.

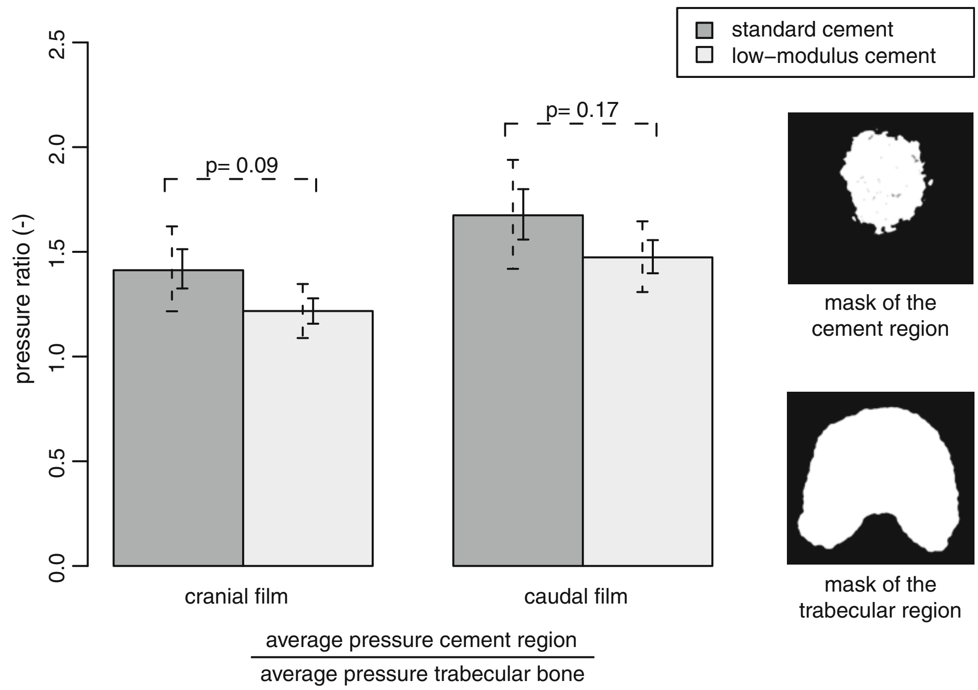


**Fig. 9** Ratio between the averaged pressure inside the cement (*right*, *top*) and trabecular region mask (*right*, *bottom*) for standard and low-modulus cement

## Discussion

Apparent stiffness, strength, and endplate pressure distribution were compared between augmentation with a clinically used standard cement and with an experimental low-modulus cement in consideration of filling patterns. Stiffness was compared to the non-augmented state and strength to a reference group.

Endplate-to-endplate fillings increased stiffness significantly for both cements compared to the non-augmented state and increased strength significantly compared to the non-augmented control group. Apparent strength was smaller with low-modulus cement compared to standard cement, but further studies are required for sufficient statistical power. Partial fillings caused less alteration of the stress transfer, but were not able to increase strength with both cements because the fracture occurred above or below the cement.

Increase in strength for endplate-to-endplate fillings (47% with standard cement and 30% with low-modulus cement) were similar to previous findings for prophylactic vertebroplasty (37% in [20] and 38% in [18]). Other studies reported larger strength and stiffness increases (factor of 2.0–7.8 for stiffness increase and 1.2–11.1 for strength increase in [15]; 174% increase in stiffness and 195% increase in strength in [19]), but cement volumes in these studies were much larger (7.5–10.5 ml in [15] and 5–20 ml in [19]). The larger increases in strength and stiffness for endplate fillings compared to partial fillings were comparable to [15], where only minimal strengthening (<20%) was observed for partial fillings. Differences in strength increases between the filling groups were also similar to previous studies (e.g., 40% difference in [25]).

The injected cement volumes varied between 1.9 and 6.0 ml and were similar to clinically used amounts reported in [11] (average 4.1 ml, ranging from 1.0 to 9.0 ml). Cement volumes were significantly higher in the low-modulus cement group due to better injectability, longer handling, and better coherence which reduced the occurrence of leakage. In fact, the macroscopic stiffness differences between the two cement groups may not reflect the 2.3 times higher stiffness of the standard cement.

Good correlations were found between BV/TV and apparent stiffness after augmentation for both cement groups, which agreed with previous results [16]. Apparent stiffness before and after augmentation were predicted by BV/TV with comparable $R^2$ but different regression equations. These correlations show that the pre-existing bone quality has a strong influence on the stiffness outcome because a part of trabecular structure is reinforced.

The presence of stiff cement increased the endplate pressure above/below the cement compared to the trabecular region in case of endplate fillings. This effect was reduced with low-modulus cement (on average 15%), although not significantly. The pressure distributions showed that the cement transmitted stresses between both endplates. This explains why endplate-to-endplate fillings were more effective than partial fillings in increasing apparent strength and stiffness, and confirms the importance of this bridging mechanism [15, 25]. The pressure concentrations above/below the cement correspond to a high local stiffness and, inversely, to a low deflection of the endplate. The pressure distributions were in line with endplate deflection patterns observed in [26]. High pressures corresponded to low deflections of the endplate. Possible consequences are an increased pressure in the nucleus pulpous, an altered stress transfer to the adjacent level [10, 11], and unloading of the surrounding bone leading to resorption. In case of partial fillings, no such pressure concentrations occurred. Although this may reduce the above-mentioned negative effects, strength was not increased due to the missing endplate bridging. Thus, a compromise could be the augmentation from endplate-to-endplate with low-modulus cement, but further studies are necessary to determine optimal cement material properties.

This study had the following limitations. First, the experimental setup was not able to reproduce in vivo loading and boundary conditions exactly because of missing endplates and intervertebral disks. However, using vertebral sections minimized errors due to the compliances embedding and the interface between bone and embedding. Eswaran et al. [27] showed that vertebral body sections captured the load-sharing variations qualitatively, but quantitatively overestimated the maximum shell-load fraction (21% on average). Second, the number of specimens with partial fillings was rather small ($N = 3$), but strength increases were similar for all eight specimens with this filling pattern because damage localized in the non-augmented part. Third, the specimens were augmented in vitro. Fourth, the study was limited to prophylactic vertebroplasty, which is not widely accepted although recent studies [28, 29] showed a reduced risk of new fractures.

In conclusion, the present study showed that the low-modulus cement was able to significantly increase strength and stiffness of vertebral body sections, but, endplate-to-endplate fillings were required with both cements to increase structural properties. This confirms the importance of the bridging mechanism, which allows stress transmission between both endplates. Pressure concentrations above/below the endplates were smaller with low-modulus cement compared to standard cement. However, further studies are required to investigate if this reduction of pressure concentrations is sufficient to reduce complications.

**Acknowledgments** The authors acknowledge the AO Research Foundation for grant support, Synthes GmbH for providing the cement and injection kits, Prof. Klaus Hoffmann (IKL, Vienna University of Technology) for providing the software GODAV, Prof. Paul Heini (Sonnenhofklinik, Bern, Switzerland) for his clinical expertise, Thomas Bandur for preparation the vertebral bodies and Christoph Messner for assistance in the laboratory. Special thanks to Enrico Dall'Ara for fruitful discussion and advice with specimen preparation and mechanical testing.

**Conflict of interest** None.

## References

1. Belkoff SM, Mathis JM, Jasper LE, Deramond H (2001) The biomechanics of vertebroplasty. The effect of cement volume on mechanical behavior. Spine 26(14):1537–1541
2. Liebschner MA, Rosenberg WS, Keaveny TM (2001) Effects of bone cement volume and distribution on vertebral stiffness after vertebroplasty. Spine 26(14):1547–1554
3. Serra L, Mehrabi Kermani F, Panagiotopoulos K, De Rosa V, Vizioli L (2007) Vertebroplasty in the treatment of osteoporotic vertebral fractures: results and functional outcome in a series of 175 consecutive patients. Minim Invasive Neurosurg 50:12–17
4. Grados F, Depriester C, Cayrolle G, Hardy N, Deramond H, Fardellone P (2000) Long-term observations of vertebral osteoporotic fractures treated by percutaneous vertebroplasty. Rheumatology 39:1410–1414
5. Uppin AA, Hirsch JA, Centenera LV, Pfiefer BA, Pazianos AG, Choi IS (2003) Occurrence of new vertebral body fracture after percutaneous vertebroplasty in patients with osteoporosis. Radiology 226(1):119–124
6. Berlemann U, Ferguson SJ, Nolte LP, Heini PF (2002) Adjacent vertebral failure after vertebroplasty. A biomechanical investigation. J Bone Joint Surg Br 84(5):748–752
7. Boger A, Heini PF, Windolf M, Schneider E (2007) Adjacent vertebral failure after vertebroplasty: a biomechanical study of low-modulus PMMA cement. Eur Spine J 16(12):2118–2125
8. Nouda S, Tomita S, Kin A, Kawahara K, Kinoshita M (2009) Adjacent vertebral body fracture following vertebroplasty with polymethylmethacrylate or calcium phosphate cement: biomechanical evaluation of the cadaveric spine. Spine 34(24): 2613–2618
9. Klazen CAH, Venmans A, de Vries J, van Rooij WJ, Jansen FH, Blonk MC, Lohle PNM, Juttmann JR, Buskens E, van Everdingen KJ, Muller A, Fransen H, Elgersma OE, Mali WPThM, Verhaar HJJ (2010) Percutaneous vertebroplasty is not a risk factor for new osteoporotic compression fractures: results from VERTOS II. Am J Neuroradiol 31:1447–1450
10. Baroud G, Nemes J, Heini PF, Steffen T (2003) Load shift of the intervertebral disc after a vertebroplasty: a finite-element study. Eur Spine J 12(4):421–426
11. Polikeit A, Nolte LP, Ferguson SJ (2003) The effect of cement augmentation on the load transfer in an osteoporotic functional spinal unit: finite-element analysis. Spine 28(10):991–996
12. Banse X, Sims TJ, Bailey AJ (2002) Mechanical properties of adult vertebral cancellous bone: correlation with collagen intermolecular cross-links. J Bone Miner Res 17:1621–1628
13. Kühn KD (2000) Bone Cements. Up-to-date comparison of physical and chemical properties of commercial materials, vol 1. Springer, Berlin
14. Boger A, Bohner M, Heini PF, Schwieger K, Schneider E (2008) Performance of vertebral cancellous bone augmented with compliant PMMA under dynamic loads. Acta Biomater 4:1688–1693
15. Chevalier Y, Pahr DH, Charlebois M, Heini PF, Schneider E, Zysset PK (2008) Cement distribution, volume, and compliance in vertebroplasty: some answers from an anatomy-based nonlinear finite element study. Spine 33(16):1722–1730
16. Graham J, Ahn C, Hai N, Buch BD (2007) Effect of bone density on vertebral strength and stiffness after percutaneous vertebroplasty. Spine 32(18):505–511
17. Dall'Ara E, Schmidt R, Pahr DH, Varga P, Patsch J, Chevalier Y, Kainberger F, Zysset PK (2010) A nonlinear finite element model

validation study based on a novel experimental technique for inducing anterior wedge-shape fractures in human vertebral bodies in vitro. J Biomech 43(12):2374–2380
18. Furtado N, Oakland RJ, Wilcox RK, Hall RM (2007) A biomechanical investigation of vertebroplasty in osteoporotic compression fractures and in prophylactic vertebral reinforcement. Spine 32(17):480–487
19. Heini PF, Berlemann U, Kaufmann M, Lippuner K, Fankhauser C, van Landuyt P (2001) Augmentation of mechanical properties in osteoporotic vertebral bones—a biomechanical investigation of vertebroplasty efficacy with different bone cements. Eur Spine J 10(2):164–171
20. Higgins KB, Harten RD, Langrana NA, Reiter MF (2003) Biomechanical effects of unipedicular vertebroplasty on intact vertebrae. Spine 28(14):1540–1547
21. Boger A, Wheeler K, Montali A, Gruskin E (2009) NMP-modified PMMA bone cement with adapted mechanical and hardening properties for the use in cancellous bone augmentation. J Biomed Mater Res B Appl Biomater 90(2):760–766
22. Laib A, Rüegsegger P (1999) Comparison of structure extraction methods for in vivo trabecular bone measurements. Comput Med Imaging Graph 23:69–74
23. Pahr DH, Zysset PK (2009) From high-resolution CT data to finite element models: development of an integrated modular framework. Comput Meth Biomech Biomed Eng 12:45–57
24. Leng L, Zhang T, Kleinman L, Zhu W (2007) Ordinary least squares regression, orthogonal regression, geometric mean regression and their application in aerosol science. J Phys Conference Series 78:012084–012088
25. Steens J, Verdonschot N, Aalsma AMM, Hosman AJF (2007) The influence of endplate-to-endplate cement augmentation on vertebral strength and stiffness in vertebroplasty. Spine 32(15): 419–422
26. Hulme PA, Boyd SK, Heini PF, Ferguson SJ (2009) Differences in endplate deformation of the adjacent and augmented vertebra following cement augmentation. Eur Spine J 18(5):614–623
27. Eswaran SK, Gupta A, Adams MF, Keaveny TM (2006) Cortical and trabecular load sharing in the human vertebral body. J Bone Miner Res 21(2):307–314
28. Kobayashi N, Numaguchi Y, Fuwa S, Uemura A, Matsusako M, Okajima Y, Ishiyama M, Takahashi O (2009) Prophylactic vertebroplasty: cement injection into non-fractured vertebral bodies during percutaneous vertebroplasty. Acad Radiol 16(2):136–143
29. Diel P, Freiburghaus L, Röder C, Benneker LM, Popp A, Perler G, Heini PF (2011) Safety, effectiveness and predictors for early reoperation in therapeutic and prophylactic vertebroplasty: short-term results of a prospective case series of patients with osteoporotic vertebral fractures. Eur Spine J. doi:10.1007/s00586-011-1989-x